Implementation of the Huygens Absorbing Boundary Condition in Corner Regions

Fumie Costen, *Member, IEEE*, and Jean-Pierre Bérenger, *Fellow, IEEE*

Abstract—In recent years, three new absorbing boundary conditions (ABCs) have appeared in the literature, namely, the multiple absorbing surfaces, the reradiating boundary condition, and the Huygens ABC (HABC). The last is a generalization of the first two. The HABC mainly relies on the radiation of a field opposite to the outgoing field by means of surface currents. This paper focuses on the implementation of the HABC in the corner regions of computational domains. It is shown rigorously that the Huygens surface radiating the opposite field is not a normal Shelkunoff surface. Additional branches, called extensions, must be added in the corner regions.

Index Terms—Absorbing boundary condition (ABC), finite difference, finite-difference time-domain (FDTD) method, Huygens surface.

I. INTRODUCTION

TWO novel absorbing boundary conditions (ABCs) were presented independently some years ago in the literature: the multiple absorbing surfaces [1] and the reradiating boundary condition (rRBC) [2], [3]. Both rely on the same principle of canceling the outgoing field leaving a computational domain by means of equivalent currents that radiate a field equal in magnitude and opposite in sign to the field to be cancelled. This concept has been generalized and investigated in details in [4], where it is called the Huygens ABC (HABC).

As shown in [4], the HABC is equivalent to a traditional operator ABC. This is because the HABC concept cannot be implemented rigorously. More precisely, the required equivalent currents are not known on the boundary where they must be applied so that they are replaced with an estimate computed using an operator, for example a Higdon operator [5], [6]. However, the HABC is not just another implementation of traditional operator ABCs [4]. First, it can be easily designed to absorb evanescent waves [4]. Second, it can be combined with such other ABCs as the PML ABC [4] or a real stretch of coordinates [7]. For these reasons, and since in addition it is simpler than the PML ABC, the HABC is a promising ABC that may challenge the well-established PML ABC in some problems, or can be used to improve the effectiveness of other ABCs.

The papers [1]–[4] mainly present the principle and the theory of the proposed ABCs on a plane boundary assumed as of infinite extent. Although numerical experiments are reported in these papers in two or three dimensions, little attention is paid to the corners of the computational domain. By contrast, this paper focuses precisely on this question, which is a critical question since the equivalent currents that generate the opposite wave are not just a usual Huygens surface.

As stated by the Shelkunoff theorem, a Huygens surface is a closed and continuous surface that splits the physical space into two regions, in general an interior region and an exterior region. Sources in one region can be replaced with equivalent currents that radiate the same field as the sources into the other region. Huygens surfaces are currently used with the finite-difference time-domain (FDTD) method either to generate an incident wave or for the near-to-far field transformation [8]. In Cartesian coordinates, they take the form of a parallelepiped. In the HABC [4] and in its special cases [1] and [2], [3], the situation is more complex. The reason is that the exact equivalent currents are replaced with estimates computed with an operator that is discontinuous at the corners of the HABC. If a normal Huygens surface is used, the radiated field is discontinuous so that spurious sources are produced in the corners. To overcome this problem, additional surfaces must be added to the Huygens surface. They extend from the corners or edges to the outer end of the computational domain. We call them the extensions of the Huygens surface.

In papers [1] and [2], [3], the need for extensions is not discussed and even mentioned. However, there is some evidence, as in Fig. 6 in [1] or in Table I in [3], that the Huygens planes were extended up to the outer boundary ending the domain. In other words, what we call here extensions were used in the numerical experiments. The rationale for the authors to do this is not reported. It may be a proper understanding of the corner problem or the simplification of the implementation suggested by a brief comment in [1]. Thus, in view of future developments of the HABC, there is a need for clarification and a proper theoretical justification of the implementation in the corners. This is the purpose of the present paper. It shows in detail why the extensions are needed and reports some numerical experiments that demonstrate the impact of the extensions on the correctness of the computed results. The absence of extension has a limited impact on the results when the HABC is set closely to the outer boundary ending the domain, as in the experiments in [1]–[4], but when the space between the HABC and the outer boundary is large, as in the method [7], the presence of the extensions is primordial. Without extension, the computed results are strongly erroneous.
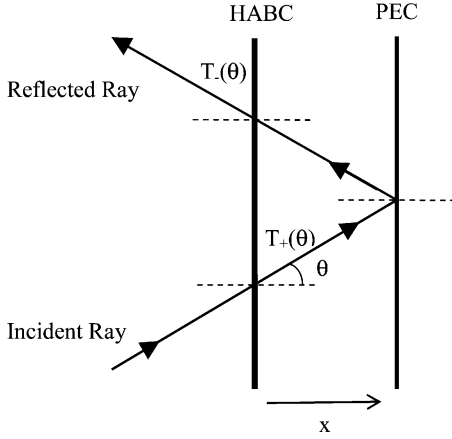
Fig. 1.　A plane wave propagating toward an infinite wall HABC.

The content of this paper is as follows. Section II summarizes the properties of the HABC [4] on a wall boundary. Section III shows that the field radiated by a normal Huygens surface is discontinuous in the corner regions of the HABC. Section IV presents the extended HABC which removes the discontinuity. Section V shows several experiments in the 2-D case to illustrate the theory. Finally, Section VI briefly illustrates the effectiveness of the combination of the HABC with a stretch of coordinates [7] to solve some typical open problems of electromagnetic compatibility.

II. HABC ON A WALL BOUNDARY

Let us consider a plane HABC placed in front of a plane perfect electric conductor (PEC), with an incident wave propagating at an angle of incidence θ. This is a 3-D problem depicted in Fig. 1 looking along the plane of incidence. From [4], the estimate of the field at the HABC location can be written as follows:

$$\tilde{U}(x_{\text{HABC}}, t) = \sum_{k=1}^{M} a_k U(x_{\text{HABC}} - \delta x_k, t - \delta t_k)$$
$$+ \sum_{k=M+1}^{N} a_k \tilde{U}(x_{\text{HABC}}, t - \delta t_k) \quad (1)$$

where U is either the E or H field, and $\tilde{U}$ is the estimate of U. The first term is a linear function of U at M interior locations $x_{\text{HABC}} - \delta x_k$ and previous times $t - \delta t_k$. The second term is a combination of $N - M$ estimates at previous times $t - \delta t_k$. When an incident wave $U_{i+}(t)$ comes from the left-hand side, from [4] the wave $U_{t+}(t)$ transmitted by the HABC, i.e., the field to the right of the HABC if the PEC were absent, is the derivative on time of the incident wave:

$$U_{t+}(t) = T_+(\theta) \frac{\partial U_{i+}(t)}{\partial t} \quad (2)$$

with

$$T_+(\theta) = \frac{1}{1 - \sum_{k=M+1}^{N} a_k} \sum_{k=1}^{N} a_k \left(\delta t_k - \frac{\cos \theta \delta x_k}{c} \right) \quad (3)$$

where c is the speed of light. We assume that the numerical technique is the FDTD method [8] so that the shifts in space and time δx_k and δt_k are multiples of the steps on space and time Δx and Δt, respectively. We use the first-order Higdon operator with which the estimate reads:

$$\tilde{U}^{n+1}(I_{\text{HABC}}) = U^n(I_{\text{HABC}} - 1) + w\, U^{n+1}(I_{\text{HABC}} - 1)$$
$$- w\tilde{U}^n(I_{\text{HABC}}) \quad (4)$$

where n is the index on time, I is the index on space in x direction, and

$$w = \frac{c\Delta t - \Delta x}{c\Delta t + \Delta x}. \quad (5)$$

The estimation (4) is a special case of (1) with $M = 2$ and $N = 3$. Using (1), (3), and (4), the coefficient $T_+(\theta)$ of the Higdon operator is obtained as follows:

$$T_{+\text{Hig}}(\theta) = \frac{1}{1 + w} \left[(1 - w)\Delta t - \frac{\cos \theta\, (1 + w)\Delta x}{c} \right]$$
$$= \frac{(1 - \cos \theta)\, \Delta x}{c}. \quad (6)$$

Consider now a wave $U_{i-}(t)$ propagating from the right-hand side of the HABC, such as the reflected ray in Fig. 1. From [4], the wave $U_{t-}(t)$ transmitted to the left-hand side of the HABC is the integral on time of $U_{i-}(t)$:

$$U_{t-}(t) = T_-(\theta) \int_{-\infty}^{t} U_{i-}(t')dt' \quad (7)$$

with

$$T_-(\theta) = \frac{1 - \sum_{k=M+1}^{N} a_k}{\sum_{k=1}^{N} a_k(\delta t_k + \cos \theta\, \delta x_k/c)} \quad (8)$$

or in the special case of the Higdon operator:

$$T_{-\text{Hig}}(\theta) = \frac{1+w}{[(1-w)\Delta t + \cos \theta(1+w)\Delta x/c]} = \frac{c}{(1+\cos \theta)\Delta x}. \quad (9)$$

For the problem in Fig. 1, the incident wave is differentiated by the HABC and transmitted with the coefficient $T_+(\theta)$, reflected from the PEC with the coefficient -1, and then integrated by the HABC and transmitted back into the interior domain with the coefficient $T_-(\theta)$. The net result is the apparent reflection:

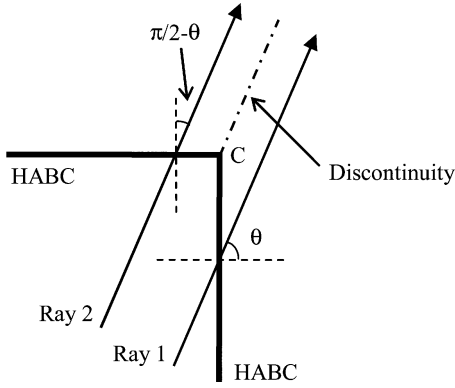$$R(\theta) = -T_-(\theta)T_+(\theta) \quad (10)$$

Fig. 2.   Discontinuity of the transmitted wave at the corner of a 2D HABC.

Fig. 3.   The extensions of the HABC at the corners in the 2D case.

where a term corresponding to the free space propagation between HABC and PEC has been omitted. For pure traveling waves, this term is a phase term of modulus one. For evanescent waves, it would equal the natural decay of the wave. As shown in [4], the reflection (10) equals, rigorously, the reflection obtained by enforcing the estimate (1) as a boundary condition. This is easily verified in the case of the Higdon operator, where using (6), (9), and (10), we obtain $R(\theta) = -(1 - \cos\theta)/(1 + \cos\theta)$, which is the well-known reflection from the first-order Higdon operator [5], [6]. Therefore, the ABC composed of a HABC surface and a PEC surface is equivalent, rigorously, to the corresponding operator ABC.

III. HABC AT THE EDGES AND CORNERS OF A COMPUTATIONAL DOMAIN

Let us first consider the 2-D case depicted in Fig. 2, where an HABC without PEC behind it radiates the wave opposite to the incident wave. Assume that the outgoing wave is a plane wave at incidence θ with respect to the vertical in Fig. 2, and consider two rays that strike the HABC to the right and to the left of the corner C. Then the incidence on the Huygens surface is θ for ray 1 and $\pi/2 - \theta$ for ray 2. The transmitted waves corresponding to the two rays are the derivative on time of the incident wave, multiplied with the coefficients $T_+(\theta)$ and $T_+(\pi/2 - \theta)$, respectively, where T_+ is given by (3) in general or (6) in the special case of the Higdon operator. It is obvious from (3) or (6) that the magnitudes of the two transmitted rays are different, except in the case where $\theta = \pi/4$. This is true for all rays as long as they strike the HABC on the two sides of the corner C, and whatever may be their distance from C. Thus, the transmitted field is discontinuous behind the HABC. The wave is no longer a plane wave. Its magnitude varies in the direction perpendicular to the propagation. This also occurs in 3-D at the edges of the HABC, which are similar to 2-D corners, and at the 3-D corners, where there are three different transmission coefficients. In both 2- and 3-D, such discontinuities produce additional components to the field, i.e., they act as spurious sources.

The discontinuity in the transmitted wave originates in the estimate of the opposite field radiated by the Huygens surface. If the exact outgoing field was 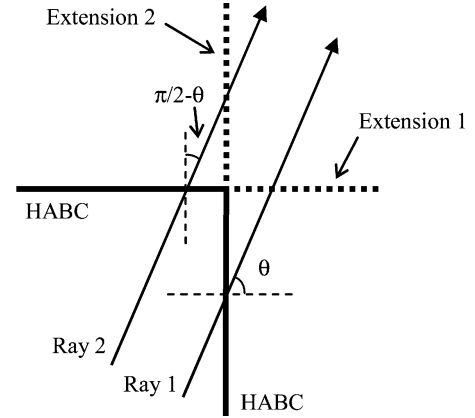used as equivalent current, the radiated field would be exact. With the HABC, the unknown outgoing field is replaced with an estimate computed using an operator that depends on the incidence on the Huygens surface. At the corner, the operator and then the estimates (3) or (6) are discontinuous simply because the incidence angle experiences an abrupt change, from θ to $\pi/2 - \theta$ in the 2-D case in Fig. 2. This results in a discontinuity in the radiated field that produces a nonphysical source that may be very large, as demonstrated by a numerical experiment in the Section V.

IV. EXTENDED HABC

A simple modification of the Huygens surface permits the discontinuity in the transmitted field to be removed. Let us first consider the 2-D case. The modification is depicted in Fig. 3. It consists of extending the HABC surfaces (reduced to lines in 2-D) up to infinity in theory or up to the end of the computational domain in practice. The equivalent currents on the extensions are enforced as on the normal HABC surfaces. For instance, the equivalent currents on extension 1 are computed using the same operator as on the normal horizontal HABC and are enforced by means of the same modifications to the Maxwell equations.

With the extended HABC in Fig. 3, ray 1 crosses the vertical HABC, where it is differentiated on time and transmitted with coefficient $T_+(\theta)$. Then it crosses extension 1, where it is differentiated another time and transmitted with $T_+(\pi/2 - \theta)$. Similarly, ray 2 crosses the horizontal HABC, where it is differentiated and transmitted with $T_+(\pi/2 - \theta)$, and then crosses extension 2, where it is differentiated and transmitted with $T_+(\theta)$. In the region in-between the two extensions, the two transmitted waves are the second derivative of the incident wave and their magnitudes are equal to $T_+(\theta) \, T_+(\pi/2 - \theta)$. Thus, in this region, the discontinuity of the field is removed and the field remains a plane wave.

In summary, the space outside the HABC is split into three regions. Two regions where the field is the first derivative on time, separated by the region where the field is the second derivative on time. The field is a true plane wave in each region. As verified by numerical experiments in Section V, no spurious source is present.
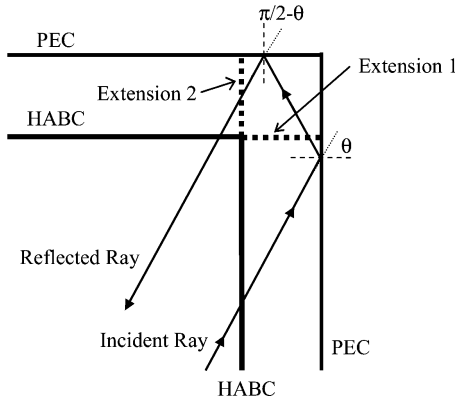
Fig. 4.   Reflection of a plane wave from the corner of an extended HABC.
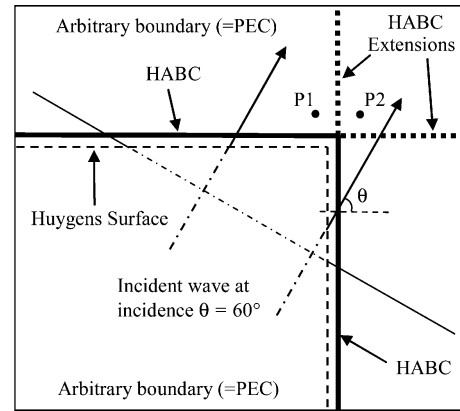

Fig. 5.   Numerical experiments with a plane wave striking a corner of the HABC. The spatial and time steps of the 2D FDTD domain are 5 cm and 100 ps, respectively.

Fig. 3 and the aforementioned derivations address the 2-D case. In 3-D, there are edge regions similar to the 2-D corners. At the 3-D corners, by extending the three Huygens planes up to infinity, the space outside the HABC is split into seven regions. It can be seen that the field in all the regions is a true plane wave, without discontinuity of the transmission coefficient. In three regions the field is the first derivative of the incident wave, in three others it is the second derivative, and in the last it is the third derivative. In this seventh region, the transmission is the product of three coefficients (3) or (6) and is the same for all the rays so that the continuity of the field is ensured.

Consider now the reflection of a plane wave from the corner region when a PEC is present behind the HABC, as depicted in Fig. 4. The ray shown in Fig. 4 is differentiated and transmitted by the vertical HABC with the coefficient $T_+(\theta)$, reflected from the PEC, differentiated and transmitted by the horizontal extension 1 with $T_+(\pi/2 - \theta)$, reflected from the horizontal PEC, integrated and transmitted by extension 2 with $T_-(\theta)$, and finally integrated and transmitted by the horizontal HABC with $T_-(\pi/2 - \theta)$. The net reflection reads:

$$R_{\text{EXTcorner}} = T_+(\theta)T_+\left(\pi/2 - \theta\right) T_-(\theta)\, T_-\left(\pi/2 - \theta\right).$$
(11)

Using (10), this can be rewritten as follows:

$$R_{\text{EXTcorner}}(\theta) = R_{\text{ABC}}(\theta)R_{\text{ABC}}\left(\frac{\pi}{2} - \theta\right)$$
(12)

where $R_{\text{ABC}}(\theta)$ and $R_{\text{ABC}}(\pi/2 - \theta)$ are the reflections from the operator ABC on the vertical and horizontal boundaries, respectively. From this, the reflection from the corner of the HABC is identical to the reflection from the corner of the domain bounded by the operator ABC relying on the same operator as the HABC. Obviously this is not true in the absence of extensions, since then the coefficients $T_+(\pi/2 - \theta)$ and $T_-(\theta)$ are missing in (11) so that the reflection differs from the reflection from the corner of an operator ABC (12). The presence of the extensions permits the discontinuity to be removed in the corner, and renders the HABC equivalent, rigorously, to the corresponding operator ABC.

Fig. 4 addresses the 2-D case. In 3-D, the three Huygens planes are extended up to the PEC. The reflection from the HABC corners is then the product of six coefficients, which

is the generalization of (11) to 3-D. As in 2-D, this reflection equals that of the corresponding operator ABC.

The implementation of the HABC extensions in a computer code is simple. Since the equivalent sources on the extensions are identical to those on the normal HABC surfaces, the only thing to do is a change of the limits of the loops where the equivalent currents are enforced. This is apparently what was done with the rRBC from the Table I in [3].

In principle, the extended HABC could be used with other outer boundaries than the PEC, so as to combine the HABC with another ABC [4]. At least with operator ABCs which use only nodes located in the direction perpendicular to the ABC. This is the case with Higdon operators, but not with Engquist–Majda ABC [9], which uses FDTD nodes in the transverse direction. With the PML ABC, we think that the extension of the HABC is possible as well by using extensions up to the PEC ending the PML.

Only homogeneous waves have been considered previously. However, the results and conclusions in [4] also apply to nonhomogeneous waves. Thus, the derivations and conclusions about the corner regions are also valid for evanescent waves, i.e., the extensions are also needed with evanescent waves. This is illustrated in Section V by an experiment with a scattering structure surrounded with strongly evanescent fields.

V. NUMERICAL EXPERIMENTS

This section reports two experiments which validate the theory in the previous section, and one experiment which demonstrates that the extension of the HABC is of primordial importance for further developments of the HABC technique. The experiments were performed in the 2-D case, which permits an easy generation of incident plane waves.

A. Continuity of the Field Behind the Extended HABC

In this experiment depicted in Fig. 5, a plane wave strikes the corner of a 2-D HABC. The wave is generated by means of a Huygens surface [8] placed close to the HABC. Both surfaces are truncated by nonphysical conditions so that the calculation
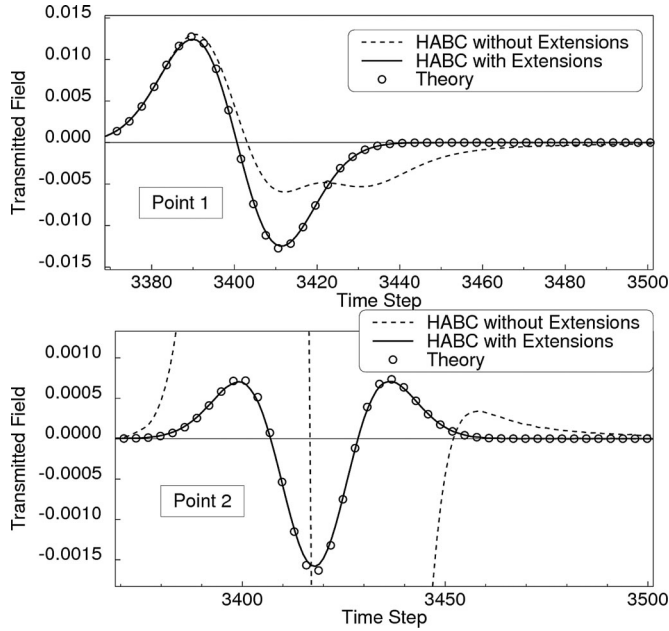
Fig. 6.   The field transmitted behind the HABC in the absence of PEC, at P1 (upper part) and P2 (lower part) in Fig. 5. Comparison of the theoretical field with the FDTD fields computed with and without HABC extensions.

Fig. 7.   Numerical experiments with a plane wave striking a corner of the HABC, with a PEC behind the HABC.

is only valid for a clear time which is about 350 time steps at the corner region with the larger than 2000 cells domain used in the experiment. The incidence is 60° with respect to the vertical ABC. The incident wave is a Gaussian pulse 15 time steps in width. The FDTD domain is large enough behind the HABC in order to ensure that the reflection from its outer boundary is not viewed in the corner region for the whole duration of the calculation.

The calculations have been performed using the HABC with and without extensions. The results are shown in Fig. 6 at the two locations denoted as P1 and P2 in Fig. 5.

At point P1, the wave should be the derivative of the incident wave multiplied with the coefficient $T_{+\text{Hig}}(\pi/2 - \theta)$. This theoretical prediction is plotted in the upper part of Fig. 6. The extended HABC result agrees very well with the theory. Without extension, the field differs from the prediction because of the discontinuity of the transmission by the HABC.

At point 2, the field with the extended HABC should be the second derivative of the incident field multiplied with $T_{+}(\pi/2 - \theta)$ and $T_{-}(\theta)$. The lower part of Fig. 6 compares this theoretical prediction with the FDTD results. The agreement is excellent with the extended HABC. Conversely, without extension the field is quite different because of the discontinuity and because it remains proportional to the first derivative so that its magnitude is about that at P1.

B. Comparison of the HABC With an Operator ABC in a Corner Region

In this experiment depicted in Fig. 7, a PEC is present 20 FDTD cells behind the HABC. As in Fig. 5, the incident wave is generated by a Huygens surface close to the HABC so that only the reflected field is present in the interior domain at the
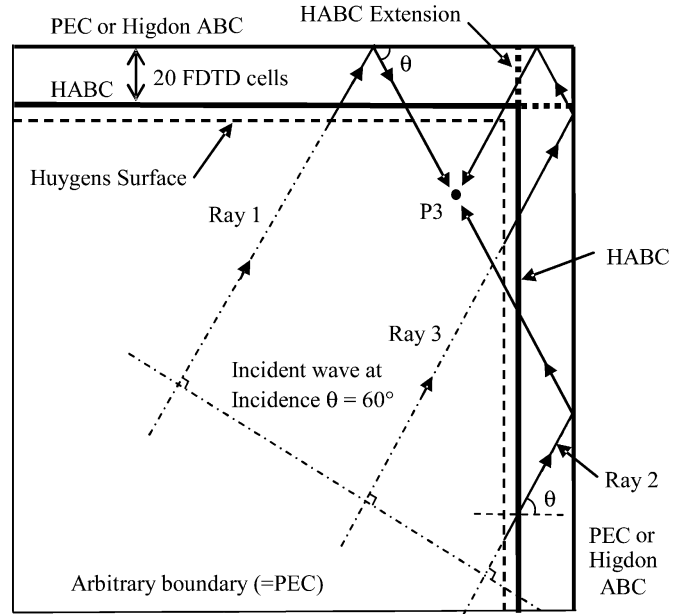
TABLE I
THE THREE CALCULATIONS WITH THE DOMAIN IN FIG. 7

Calculation	Outer boundary	HABC	HABC extension
1	PEC	yes	no
2	PEC	yes	yes
3	Higdon ABC	no	no

observation point P3. Three calculations were performed whose calculation settings are summarized in Table I. The first one with the PEC and the HABC without extension, the second one with the PEC and the HABC with extensions, and the third one without HABC and with the PEC replaced with the Higdon operator ABC. The three reflected fields at point P3 are plotted in Fig. 8, with in addition the theoretical reflection from a Higdon operator ABC.

We can observe three pulses in Fig. 8. They correspond to the three rays represented in Fig. 7. Ray 2 is the reflection from the vertical boundary with incidence θ, ray 1 from the horizontal boundary with incidence $\pi/2 - \theta$, and ray 3 from the corner. For the Higdon operator ABC and $\theta = 60°$, the corresponding reflections $R(\theta)$, $R(\pi/2 - \theta)$, and $R(\theta)$ $R(\pi/2 - \theta)$ are 0.3333, 0.0718, and 0.0239, respectively. These reflections have been used along with the differences between the ray paths to compute the theoretical reflection plotted in Fig. 8. As observed, the Higdon operator result and the extended HABC result agree very well with the expected theoretical reflection. The extended HABC is equivalent, rigorously, to the Higdon ABC. Conversely, without extensions, the HABC yields a strongly different result, the reflection from the corner (ray 3, third pulse) is one order of magnitude larger than the correct reflection, because of the
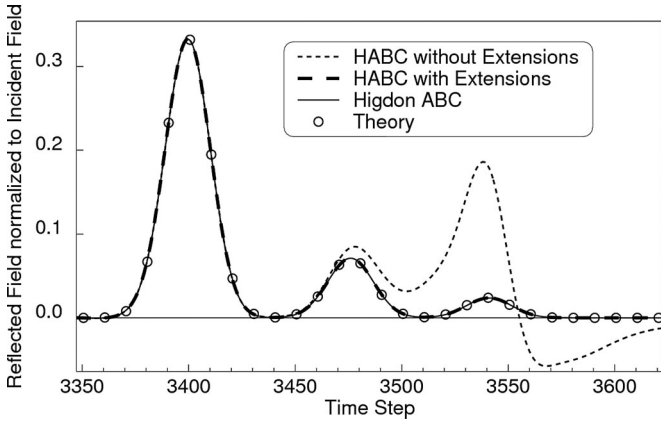
Fig. 8.   The reflected field at point P3 in Fig. 7. Comparison of the theoretical field with the results of the three FDTD calculations defined in the Table I.
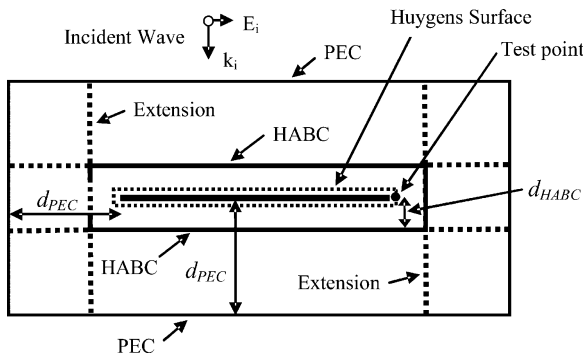

Fig. 9.   The 2D FDTD domain for the experiments with a plane wave striking a 2D 300-cell long thin plate. The FDTD steps equal 5 cm and 100 ps. The incident electric field is parallel to the PEC plate and is generated by a normal Huygens surface set 2 FDTD cells from the plate. The HABC is d_{HABC} from the plate and the outer PEC is d_{PEC} from the plate.

spurious source produced by the discontinuity of the transmitted wave.

C. Experiment With a Scattering Structure

A 300-cell-long 2-D PEC plate of zero thickness is struck by an incident plane wave propagating downward (see Fig. 9). The incident waveform is a unit step with a rise time of 10 time steps. An HABC surface and a PEC are placed at d_{HABC} and d_{PEC} from the plate, respectively. For the experiments reported in Fig. 10, the HABC surface is placed at various distances d_{HABC} from the PEC structure, ranging from 10 to 898 FDTD cells, and the PEC is 900 cells from the structure in all the calculations. Fig. 10 shows the electric field normal to the surface at the end of the plate. The HABC without extensions is used in the upper part of Fig. 10, and the extended HABC in the lower part.

As can be observed in Fig. 10, the effect of the extension is very important when the separation between the scattering structure and the HABC becomes small. Even with $d_{\text{HABC}} = 10$ cells, which is only 1/30 of the structure size, the extended HABC yields results superimposed on the solution computed with the HABC placed 900 cells away, i.e., almost superimposed on the exact solution. This means that the Higdon operator implemented as an HABC can very well absorb the traveling
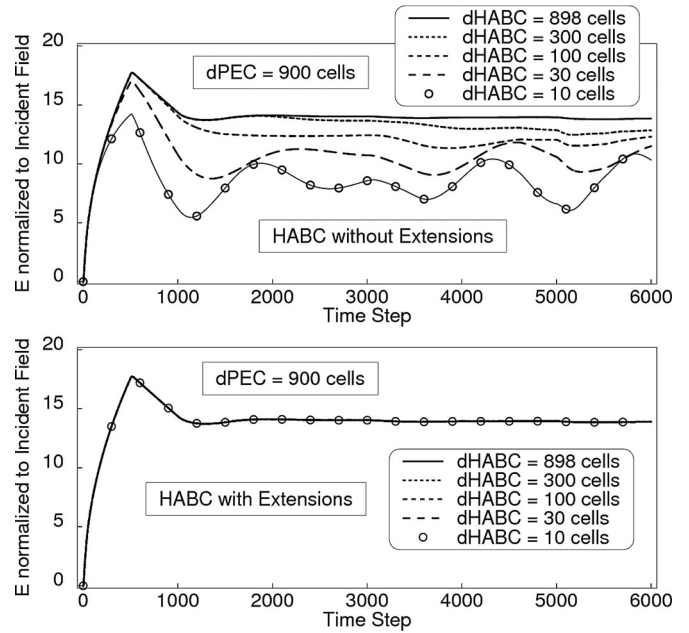

Fig. 10.   Comparison of the HABC without extension (upper part) and with the extensions (lower part) when a plane wave strikes a PEC object. The outer PEC is 900 cells from the object and the HABC is placed various distances from the object.

waves even when it is quite close to the scattering structure. Obviously, the evanescent waves are not absorbed by the HABC based on the Higdon operators [4]. In the experiments in Fig. 9, they decrease in the large space surrounding the HABC so that their apparent reflection is negligible.

VI. EFFECTIVE ABC FOR ELECTROMAGNETIC COMPATIBILITY PROBLEMS

Typical problems of electromagnetic compatibility consist of computing the field on the surface or in the vicinity of a PEC object struck by an incident wave. In such problems, the scattered field is composed of traveling waves at high frequency and evanescent waves at low frequency, with a transition about the fundamental resonance of the object. As shown above, an HABC with the Higdon operator effectively absorbs the traveling waves, even if it is close to the object. However, a large domain is still needed outside the HABC for the natural decrease of the evanescent waves.

To reduce the exterior domain, several ways can be imagined. One is the introduction of an operator designed for the evanescent waves, used either as a traditional operator ABC or in the form of an additional HABC. This was tested successfully in waveguides [4]. Another idea was introduced in [7]. It consists in keeping a large physical domain, as in Fig. 10, but with a strongly stretched FDTD mesh, so as to reduce the overall number of FDTD cells. This is possible because only the low frequency evanescent waves must be absorbed outside the HABC. Since their characteristic length of decrease is of the order of the structure size, use of quite large FDTD cells can be envisaged. This has been confirmed by experiments such as that in [7]. Thus, the combination of an HABC for the absorption
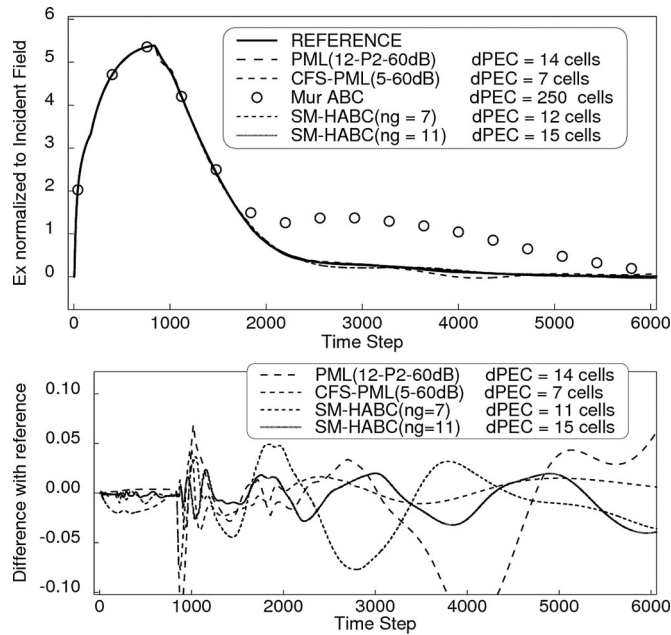
Fig. 11. Electric field at the corner on the surface of a 2D 500×50 PEC parallelepiped computed with various absorbing boundary conditions. The lower part is the difference of the computed result with the reference solution.

of the traveling waves with a stretched mesh for the absorption of the evanescent waves forms an effective ABC. We call it the Stretched Mesh HABC (SM-HABC).

A comparison of the SM-HABC with other ABCs is provided in Fig. 11 with a 2D canonical case. The incident wave is a double exponential of the form $\exp(-t/t_f)$-$\exp(-t/t_r)$ where $t_r = 1$ ns and $t_f = 100$ ns. The 2D object is a 25 m long parallelepiped of 500×50 FDTD cells of size 5 cm.

The settings of the SM-HABC calculations are similar to those in Fig. 9, with the 500×50-cell object surrounded with a HABC placed 3 cells from it, and with a large exterior domain filled with strongly stretched cells. The separation d_{PEC} between the object and the outer PEC is 75 m, that is 3 object sizes. The stretch of the mesh is a geometrical expansion that begins 4 cells from the object. Two cases are reported in Fig. 11. In the first one, the mesh is stretched upon $n_g = 7$ cells up to the outer PEC, with ratio $g = 2.68$. This means that the separation d_{PEC}, which corresponds to a physical distance of 1500 cells of 5 cm, is filled with only 11 FDTD cells. In the second case, the mesh is stretched upon $n_g = 11$ cells, with g = 1.82, so that the actual separation is $d_{\mathrm{PEC}} = 15$ cells.

Two calculations were performed with a PML ABC placed 2 FDTD cells from the object. The first one used a 12 cell thick PML with a polynomial conductivity of power 2 and the normal stretching factor. This PML is not optimum in the sense of [10], but it is probably representative of the PMLs employed by most users. The second one used the best PML which is the CFS-PML optimized for 3D wave-structure interactions [11], [12]. It is only 5 cells in thickness. Finally another result in Fig. 11 was computed with the second order Engquist-Majda ABC [9] placed 250 cells from the object.

It is clearly seen in Fig. 11 that the SM-HABC can challenge the PML ABC. Despite the extremely large cells used to fill the large domain, the accordance with the reference solution is similar to the accordance of the PML ABC. More precisely, the lower part of the figure shows that the two SM-HABCs outperform the normal 12-cell PML. Also, the magnitude of the error with the SM-HABC and $ng = 11$ cells is very close to that observed with the optimum CFS-PML. The overall number of FDTD cells is slightly larger with the SM-HABC than with the optimum CFS-PML, but the cost of one cell of vacuum is smaller than the cost of one cell of PML. Thus, the computational costs of the two ABCs are roughly similar. However, the SM-HABC has a significant advantage in comparison with the CFS-PML. Its implementation is far simpler. This is an attractive feature.

The same conclusions also hold in the 3D case. This will be demonstrated in a forthcoming paper devoted to experiments with realistic 3D scattering objects.

VII. CONCLUSION

The implementation of the HABC in the corner regions of 2D or 3D computational domains has been analysed in details. We have shown that the Huygens surface must be extended up to the surrounding PEC. The extensions that may seem in discordance with the equivalence theorem are necessary because of the replacement of the exact outgoing field with an estimate that is discontinuous at the corners of the HABC. The extensions remove the spurious sources produced by the discontinuity, and render the HABC rigorously equivalent to an operator ABC.

With the extensions the HABC is a highly effective ABC for the absorption of the travelling waves. By combining the HABC with a strategy to absorb the evanescent waves, as done in this paper with the SM-HABC, highly effective ABCs can be constructed for the solution of problems of electromagnetism, especially in the field of electromagnetic compatibility.

REFERENCES

[1] I. Wayan Sudiarta, "An absorbing boundary condition for FDTD truncation using multiple absorbing surfaces," *IEEE Trans. Antennas Propag.*, vol. 51, no. 12, pp. 3268–3275, Dec. 2003.

[2] R. E. Diaz and I. Scherbatko, "A simple stackable re-radiating boundary condition (rRBC) for FDTD," *IEEE Antenna Propag. Mag.*, vol. 46, no. 1, pp. 124–130, Feb. 2004.

[3] R. E. Diaz and I. Scherbatko, "A new multistack radiation boundary condition for FDTD based on self-teleportation of fields," *J. Comput. Phys.*, vol. 203, pp. 176–190, 2005.

[4] J.-P. Bérenger, "On the Huygens absorbing boundary conditions for electromagnetics," *J. Comput. Phys.*, 2007. doi: 10.1016/j.jcp.2007.04. 008176-190.

[5] R. Higdon, "Absorbing boundary conditions for difference approximations to the multi-dimensional wave equation," *Math. Comput.*, vol. 47, pp. 437–459, 1986.

[6] R. Higdon, "Numerical absorbing boundary conditions for the wave equation," *Math. Comput.*, vol. 49, pp. 65–90, 1987.

[7] J.-P. Bérenger and F. Costen, "Application of the Huygens absorbing boundary condition to wave-structure interaction problems," *IEEE AP-S Int. Symp.*, Toronto, Jul. 2010.

[8] A. Taflove and S. Hagness, "Computational electrodynamics: The finite-difference time-domain method," Artech House, 2005.

[9] B. Engquist and A. Majda, "Radiation boundary condition for the numerical simulation of waves," *Math. Comput.*, vol. 31, pp. 629–651, 1977.

[10] J.-P. Bérenger, "Making use of the PML absorbing boundary condition in coupling and scattering FDTD computer codes," *IEEE Trans. Electrom. Compat.*, vol. 45, no. 2, pp. 189–197, May 2003.

[11] J.-P. Bérenger, "Numerical Reflection from FDTD-PML's: A Comparison of the Split PML with the Unsplit and CFS PML's," *IEEE Trans. Antennas Propag.*, vol. 50, no. 3, pp. 258–265, Mar. 2002.

[12] J.-P. Bérenger, "The Perfectly Matched Layer for Electromagnetics," Morgan and Claypool, 2007.

Fumie Costen (M'07) received the B.Sc. degree, the M.Sc. degree in electrical engineering, and the Ph.D. degree in informatics from Kyoto University, Kyoto, Japan, in 1991, 1993, and 2005, respectively.

From 1993 to 1997, she was with Advanced Telecommunication Research International, Kyoto, where she was engaged in research on direction-of-arrival estimation based on multiple signal classification (MUSIC) algorithm for 3-D laser microvision. She received an academic invitation at Kiruna Division, Swedish Institute of Space Physics, Sweden, in 1996, and gained three patents in 1999 from the research. From 1998 to 2000, she was with Manchester Computing in the University of Manchester, Manchester, U.K., where she was engaged in research on metacomputing, and has been a Lecturer since 2000. Her research interests include computational electromagnetics in such topics as a variety of the finite-difference time-domain (FDTD) methods for microwave frequency and high spatial resolution, and FDTD subgridding and boundary conditions. Her work extends to the hardware acceleration of the computation using general-purpose computation on graphics processing units, streaming single instruction multiple data extension (SSE), and advanced vector extensions instructions.

Dr. Costen received an ATR Excellence in Research Award in 1996 and a best paper award from 8th International Conference on High Performance Computing and Networking Europe in 2000.

Jean-Pierre Bérenger (F'09) received the Master's degree in physics from the University Joseph Fourier, Grenoble, France, in 1973, and the Master's degree in optical engineering from the Institut d'Optique Graduate School, Paris, France, in 1975.

From 1975 to 1984, he was with the Département Etudes Théoriques, Centre d'Analyse de Défense, Arcueil, France, where he was engaged in research on the propagation of waves and the coupling problems related to the nuclear electromagnetic pulse. He helped popularize the finite-difference time-domain (FDTD) method in France. In 1984–1989, he was involved in the development of simulation software in the Département Nucléaire. From 1989 to 1998, he held a position as an expert on the electromagnetic effects of nuclear disturbances. He is currently a Contract Manager at the Centre d'Analyse de Défense while staying active in the field of numerical electromagnetics in topics such as VLF-LF propagation, absorbing boundary conditions, and FDTD subgridding.

Mr. Bérenger is a member of the Electromagnetics Academy. From 2006 to 2010, he was an Associate Editor of the IEEE TRANSACTIONS ON ANTENNAS AND PROPAGATION.